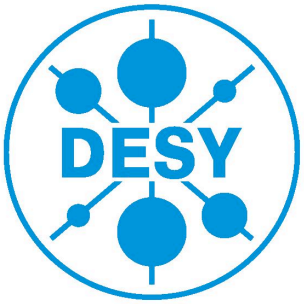

UHV Preparation and Vibrational Spectroscopic Studies on Ni(100) Surface

Yi-Xiang Liu, Peking University, Beijing

September 3, 2013

Abstract

Ni(100) sample was prepared under UHV condition. The adsorption of CO on Ni(100) at room temperature was studied by Infrared (IR) spectroscopy. Besides, the surface structure of Ni(100) before and after dosing CO was studied by Low Energy Electron Diffraction (LEED) and Auger Electron Spectroscopy (AES).

Contents

1 Introduction

Nickel is an element of atomic number 28 and has an atomic weight of 58.71. The structure of Ni single crystal is face-centered cubic (see Figure 1) with a lattice constant of 3.520 Å. The sample studied in this report is Ni(100). (100) means that the normal direction of the surface is <100> direction.

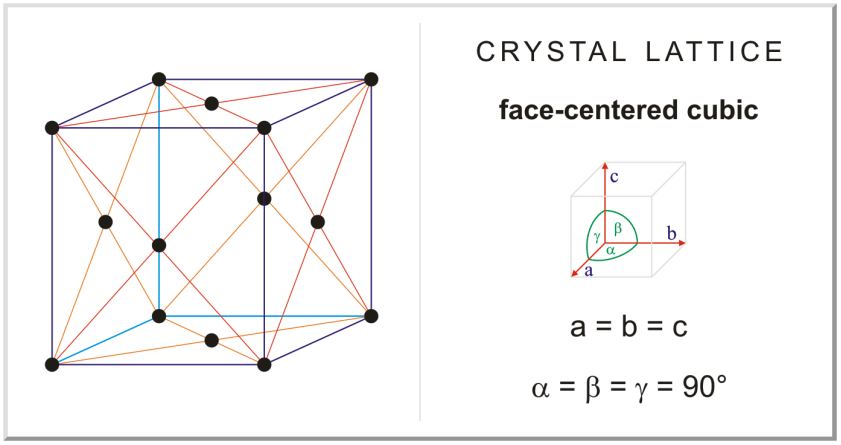

Figure 1: Crystal structure of face-centered cubic.

Nickel catalysis plays a central role in many synthetic transformations ranging from cross reactions in which carbon-carbon bonds are formed to the reduction of electron rich carbon bonds with raney catalysts. The fact that a good many of the most corrosion-resistant alloys are of nickel base or contain considerable amounts of nickel is due not only to the corrosion-resisting and strengthening characteristics of nickel itself but more importantly to the fact that nickel is metallurgically compatible over a considerable composition range with a number of other metals such as copper, chromium, molybdenum, iron, and tungsten, which have some unique corrosion-resisting properties of their own. Nickel also can serve to bring together to some extent such metallurgically immiscible metals as copper and chromium in the same alloy, so that a considerable range of compositions is available, often as a single phase alloy. These alloys frequently have the austenitic face-centered cubic structure which is commonly associated with useful engineering properties. The high tolerance of nickel for alloying without phase instability is due largely to its favorable atomic size, its nearly filled third electron shell, and its face-centered cubic lattice structure.

CO has been extensively employed as a probe molecule to monitor the nature of active sites on metal oxide surfaces. From the vibrational spectroscopy of CO adsorbed on oxide surfaces important information can be obtained about the oxidation and coordination states of the surface metal atoms.

In this report, the adsorption of CO on Ni(100) single crystal is studied considering that this system is simple and therefore to be well suited for fudndamental research on adsorption phenomena.

Figure 2: My glowing Ni(100) sample

2 Measurement and Analysis Techniques

2.1 Auger Electron Spectroscopy (AES)

Auger electron spectroscopy is an core-level spectroscopy used to study the chemical composition of surfaces. A primary electron beam with a typical energy of 2000 to 5000 eV is generated by an electron gun and accelerated onto the sample surface. The principle of an Auger process is as follows: a primary electron produces a hole in the core level of a sample atom by ionization (usually in the K or L shell). Both the primary and the core level electron leave the atom. The remaining hole in the core shell is then filled by an electron from an energetically higher-lying shell. Its energy might either be used for the emission of a characteristic X-ray photon or - as in the case of the Auger process - might be transfered to an electron in the same or a different shell. This latter Auger electron leaves the atom, is detected and its kinetic energy is analyzed. This Auger energy is dependent on the energy levels of the sample atom and can thus be used as chemical fingerprint. The nomenclature of Auger transitions reflects the core levels involved.

Electrons have a very short mean free path in solids so only Auger electrons from the topmost layers are detected. This makes AES a very surface sensitive technique with typical probing depths of 10 to 30 Å. In order to suppress the secondary electron background of the measured data, AES is usually carried out in a derivative mode $\frac{dN}{dE}$. This is performed by modulating the electron collection current via a small applied AC voltage and simultaneously detecting the signal from the electron amplifier with a lock-in amplifier[1].

2.2 Low Energy Electron Diffraction (LEED)

Low energy electron diffraction (LEED) is the oldest and probably still the most used surface crystallographic technique. It is based on the diffraction process that a monoenergetic electron beam (primary electron energy (E_p) between 20 and 500 eV)

undergos when interacting with a surface. The method is applied both to check the crystallography of the grown species and as a means of obtaining mew information of the two-dimensional periodicity of the surface. The diffraction pattern corresponds to the surface reciprocal lattice, and the reverse transformation yields the periodicity in the real space. The diffraction pattern is obtained by using a beam of electrons with a primary energy between 50 and 500 eV, at normal incident on the surface. The diffraction pattern, which is an image of reciprocal unit cell, is usually displayed on a fluorescent screen. The condition for the Bragg spot is given by the equation

$$\mathbf{K}_{\parallel} = \mathbf{k}^{'} - \mathbf{k} = \mathbf{G}_{\parallel} \tag{1}$$

where, $\mathbf{k}^{'}$ is the scattered wave vector component parallel to the surface, $\mathbf{k}$ the incident wave vector component parallel to the surface, $\mathbf{K}_{\parallel}$ the scattering vector component parallel to the surface and $\mathbf{G}_{\parallel}$ a vector of the two-dimensional surface reciprocal lattice. Equation 1 is equivalent to

$$d\, sin\phi = \lambda \tag{2}$$

where d is the spacing between two rows next to each other in real space and ϕ is the angle between the diffraction wave and the normal direction of the surface (see Figure 3). This condition is valid for the limiting case where only the topmost atomic layer is involved in scattering, In a real LEED experiment, however, the primary electrons penetrate several atomic layers into the solid and scattering events in the z-direction perpendicular to the surface contribute to the LEED pattern.

The positions of the diffraction spots, however, contain no information on the atomic positions within the unit cell. More information can be extracted from LEED data by measuring the intensity of each diffraction spot as a function of electron energy and comparing the results with a theoretical calculation. From the shape of the diffraction spots, atomic positions are derived, from the shape of the diffraction spots, long-range correlations can be detected. Such spot profiles can be employed to investigate the structural perfection of the surface providing valuable information on the steps, dislocations, facetting, mosaic width and adsorbate-adsorbate correlations[4].

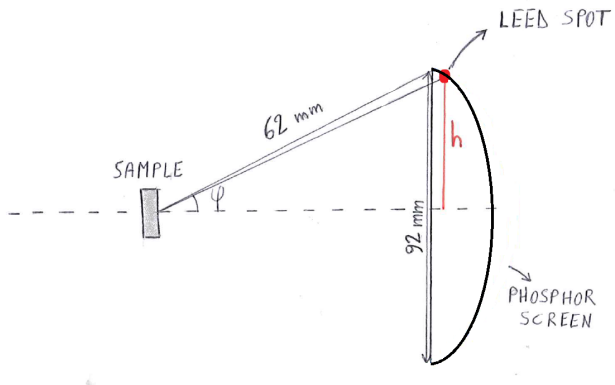

Figure 3: A simple scheme of the LEED system

2.3 Infrared (IR) Spectroscopy

In heterogeneous catalysis, IR spectroscopy has been widely used to study three main topics. The most common application is identification and characterization of adsorbed species on the catalyst surface. Moreover, IR spectroscopy can be used to identify phases in precursor states of catalysts during their preparation. The third main task is the measurement of spectra of adsorbed probe molecules such as CO or CO_2 to obtain information about the active sites present on the catalyst surface.

IR spectroscopy belongs to the field of vibrational spectroscopies. IR radiation covers a frequency range between 10 and 10000 cm^{-1} comprising far-, mid- and near-IR. The mid-IR region, ranging from 200 to 4000 cm^{-1}, is of major importance for adsorbate studies in heterogeneous catalysts, as most molecular vibrations are excited with radiation of these frequencies. In surface vibrational spectroscopy, the surface selection rule is applied to identify the peaks observed in vibrational spectra. When a molecule is observed on a substrate, it induces on opposite image charge in the substrate. The dipole moment of the molecule and the image charges perpendicular to the surface reinforce each other. In contraast, dipole moments of the molecule and the image charges parallel to the surface cancel out. Therefore only molecular vibrational peaks giving rise to a dynamic dipole moment perpendicular to the surface will be observed in the vibrational spectrum.

Physical basis for the IR spectroscopy is the transitions between discrete vibrational and rotational energy levels of molecules. Considering a diatomic molecule as the simplest example, within the model of the harmonic oscillator, the corresponding energy levels E_n are given by:

$$E_n = (n + \frac{1}{2})h\nu, \tag{3}$$

where h is the Planck constant and n is the vibration quantum number, which describes the energy level. The frequency of the vibration ν is determined by the reduced mass of the diatomic molecule, $\mu = (m_1 m_2)/(m_1 + m_2)$, and the force constant k of the bond, according to :

$$\nu = \frac{1}{2\pi}\sqrt{\frac{k}{\mu}}. \tag{4}$$

The frequency increases for the vibration of stronger bond and it decreases for molecules with heavier atoms. In the harmonic approximation, only those transitions are allowed, in which $\Delta n = \pm 1$.

A general selection rule for the observation of a band in IR spectroscopy is a change of the dipole moment of the molecule during the vibration. Symmetric molecules like N_2 cannot be observed, which is a main difference between IR and Raman spectroscopy[5].

3 Experimental

3.1 Experimental Set-ups

3.1.1 Ultra High Vacuum Chambers

All samples studied in this report were prepared in the stationary main chamber. Please see Figure 4. It is interconnected with two other chambers that are separated from the main chamber by valves. One of those is a pre-chamber that allows the loadings of samples. The other is the IR chamber (see section 3.1.2). The main chamber is pumped by a rough pump, a turbo pump and an ion getter pump which yields pressures in the UHV range of 10^{-10} mbar. It contains all devices needed for substrate preparation such as a sputter gun for substrate cleaning by Ar ion bombardment and an Auger Electron Spectroscopy (AES) and a Low Energy ELectron DIffraction (LEED) system yielding chemical information and information about the crystalline order of the surface. There is a gasline system that allows introducing gases like O_2 for the annealing process or Ar for sputtering. The samples can be heated either by a filament or additionally by means of an electron beam heater which allows temperatures above 1700K[1].

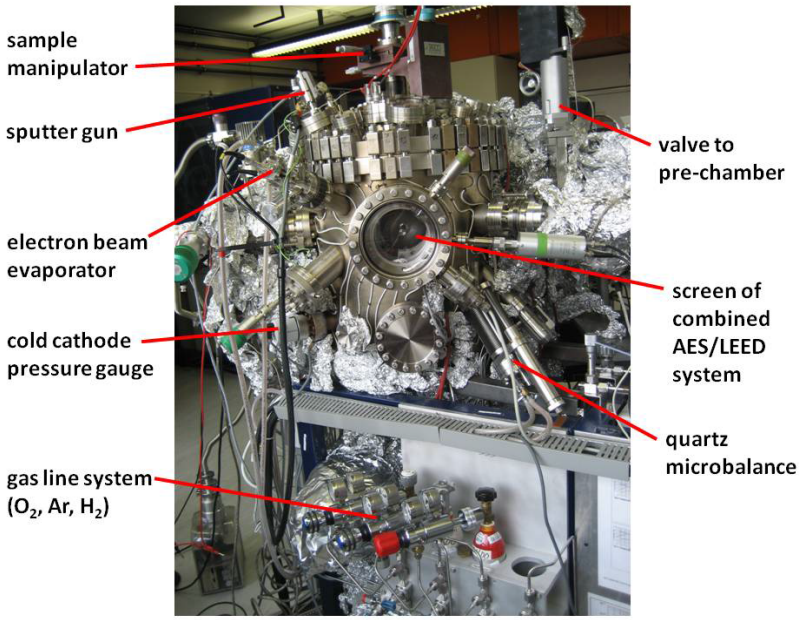

Figure 4: Main chamber. The sample studied in this report was prepared inside.

3.1.2 Ultra High Vacuum Infrared Fourier Transform Spectroscopy Apparatus Optimized for Reflection Geometries

The IR spectra in this work are obtained by employing a newly designed ultrahigh vacuum (UHV) apparatus dedicated to the spectroscopic characterization of oxides and single crystals. It combines a vacuum IR spectrometer (Bruker, VERTEX 80v, see Figure 3.1.2) with a UHV system, consisting of load-lock, distribution, measurement

and magazine chambers. In our system, the IR spectrometer is connected to a UHV chamber (this chamber is called IR chamber) and a detector is connected on the other side of the chamber (see Figure 6).

Figure 5: VERTEX 80v IR spectrometer

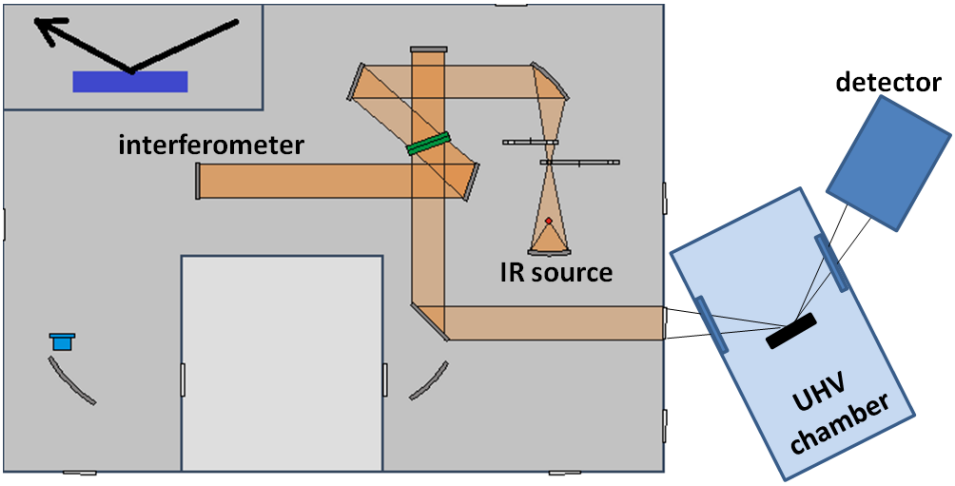

Figure 6: Scheme of reflection-absorption at grazing incidence IR measurements

3.2 Experimental Procedure

The whole procedure of the experiment is as follows:

degasing(720 K, 30 minutes) → AES → 5 cycles of sputtering and heating (sputtering:room temperature, 30 minutes; heating: 1400 K, 15 minutes) (take Auger spectra after each cycle) → transfer Ni to IR chamber → dose CO on Ni (see Table 1) → transfer Ni to the main chamber → AES and LEED → one cycle of sputtering and heating

(sputtering:room temperature, 30 minutes; heating: 1400 K, 15 minutes) → LEED and AES → transfer Ni to the IR chamber (leak, exposed to bad pressure) → transfer Ni to the main chamber → AES and LEED.

Dosing Time	CO Pressure	Langmuir
1 min	1×10^{-8} mbar	0.45
5 min	1×10^{-8} mbar	2.25
5.5 min	2×10^{-8} mbar	4.95
5.5 min	4×10^{-8} mbar	9.90
5.5 min	2×10^{-7} mbar	50
5.5 min	4×10^{-7} mbar	100
5.5 min	8×10^{-7} mbar	200

Table 1: The procedure of dosing CO on Ni(100)

4 Results

4.1 LEED Patterns and Analysis

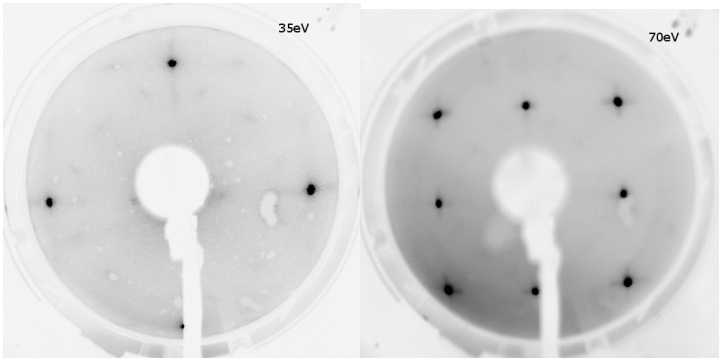

(a) Energy of the electron beam is 35 eV

(b) Energy of the electron beam is 70 eV

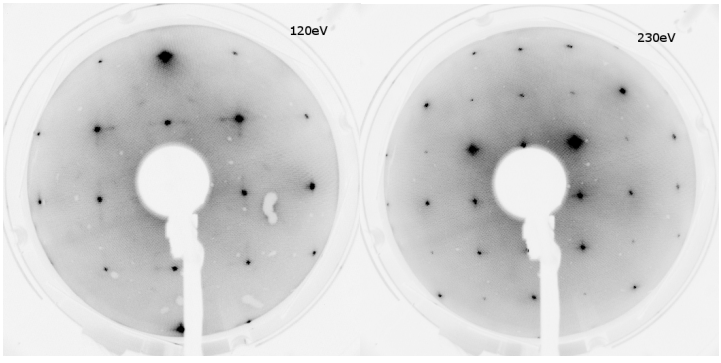

(c) Energy of the electron beam is 120 eV

(d) Energy of the electron beam is 230 eV

Figure 7: LEED patterns of Ni(100) after five cycles of sputtering and heating.

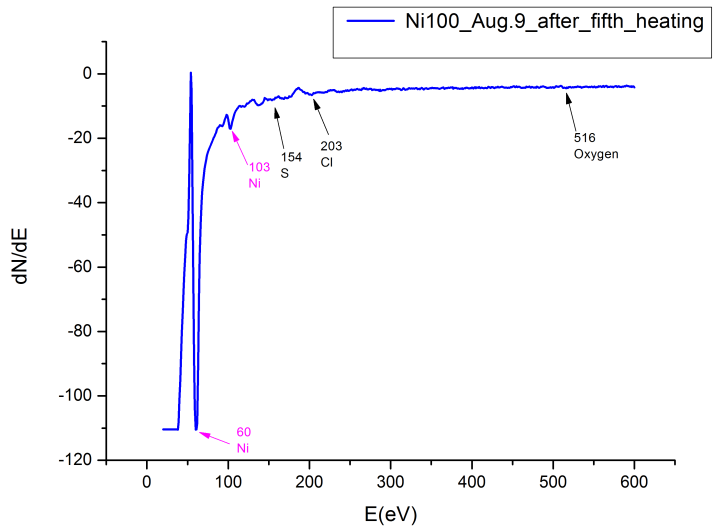

Figure 8: AES of Ni(100) after the fifth cycle of cleaning

As shown in Figure 7(a), there are four sharp spots and twelve dim spots. Using the four sharp sports to calculate the lattice constant and we can get that d spacing is 3.3 Å, which is very similasr to the lattice constant of Ni. But the largest d spacing of Ni(100) surface should be 2.5 Å. It is possible that these four spots come from c(2×2) reconstruction. The problem is what forms the reconstruction? We already know that clean Ni surface doesn't have reconstruction[2]. There are several possible impurities in nickel, such as boron, chlorine, and sulphur etc.[3]. AES can give us a better idea of what elements are on the surface. From Figure 8, except the Ni peaks, we can also see some other peaks. It is very likely that the 203 peak corresponds to Cl and Cl forms the reconstruction on the Ni surface.

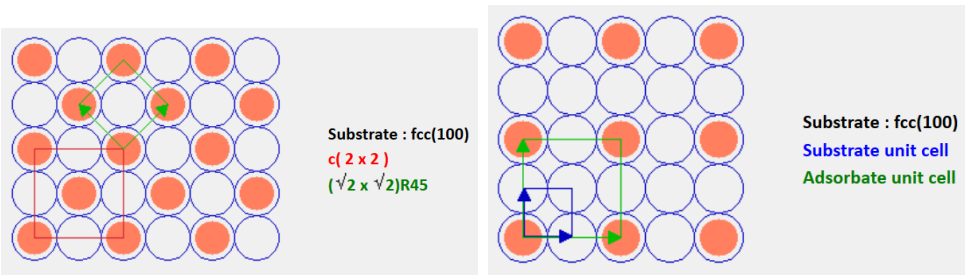

(a) c(2×2) reconstruction (b) p(2×2) reconstruction

Figure 9: Two forms of reconstruction on the fcc(100) surface

After cleaning, the sample was transfered to the IR chamber and dosed CO on the surface.

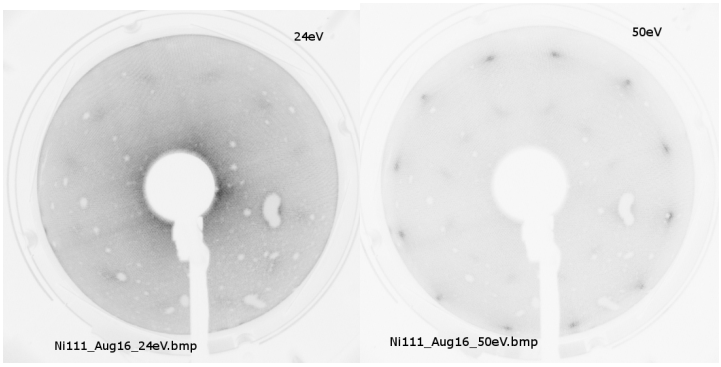

(a) Energy of the electron beam is 24 eV

(b) Energy of the electron beam is 50 eV

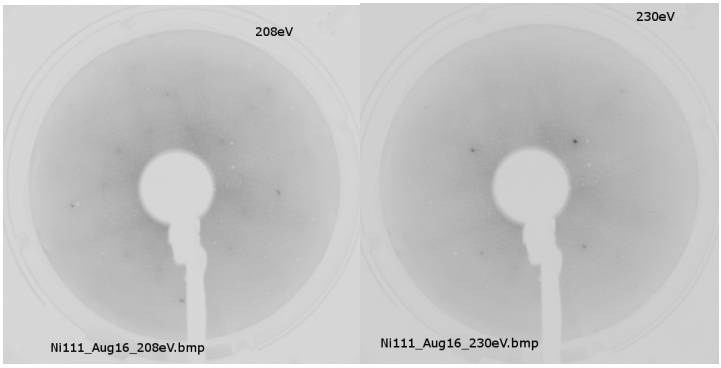

(c) Energy of the electron beam is 208 eV

(d) Energy of the electron beam is 230 eV

Figure 10: LEED patterns of Ni(100) after dosing CO

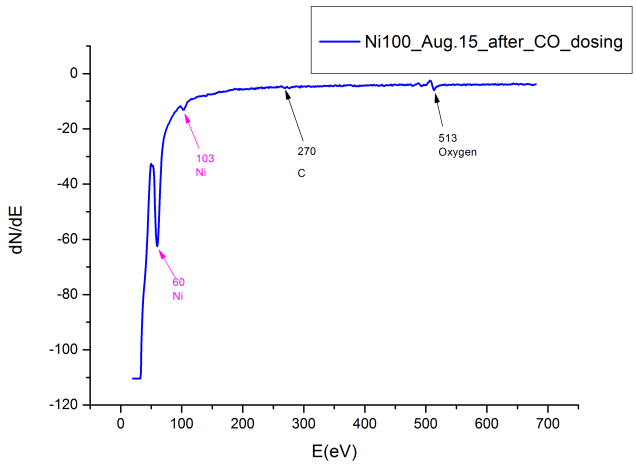

Figure 11: AES of Ni(100) after dosing CO

The LEED patterns taken after CO dosing (see Figure 11) can tell us some information about what happened on the surface of the Ni after CO dosing. When the electron energy is very low, as in Figure 10(a) and Figure 10(b), we can see a kind of twelve-fold pattern, which probably comes from a superstructure induced by well ordered CO molecules[9]. This can be confirmed by the Auger spectrum (Figure 11) taken after CO dosing. We can see intesnse oxygen peak and obvious carbon peak.

As electron energy goes higher, no clear Ni spots show up. That is because the sample surface is covered by CO molecules. While when the energy goes even higher as in Figure 10(c) and Figure 10(d), electrons can go deeper into the bulk, so we can see some sharp nickel spots.

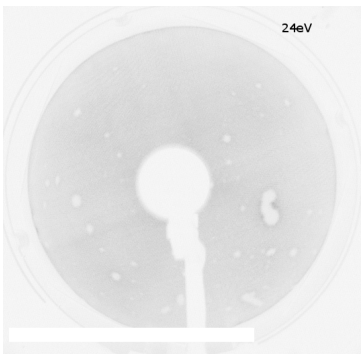

(a) Energy of the electron beam is 24 eV

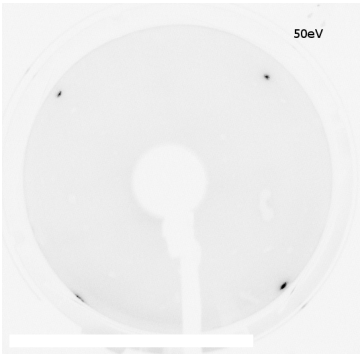

(b) Energy of the electron beam is 50 eV

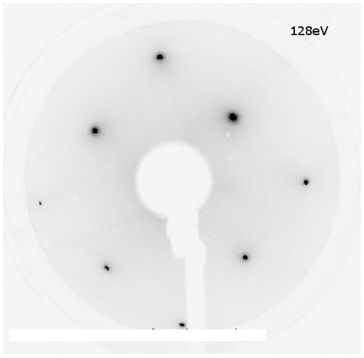

(c) Energy of the electron beam is 128 eV

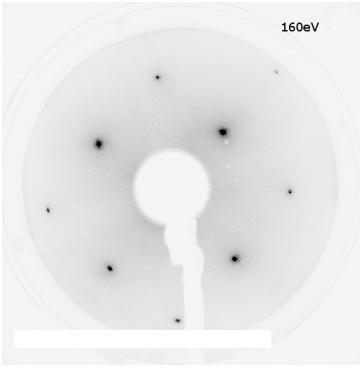

(d) Energy of the electron beam is 160 eV

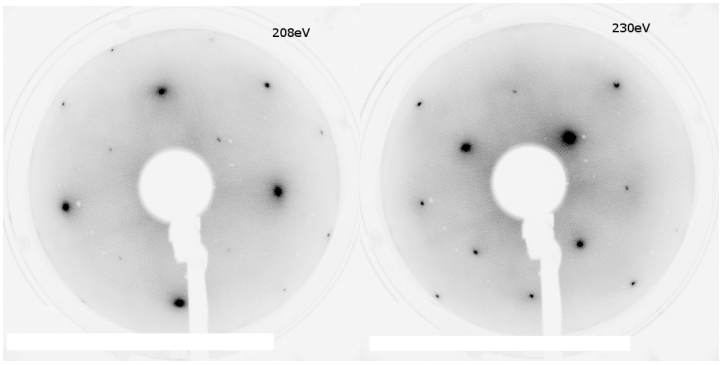

(e) Energy of the electron beam is 208 eV

(f) Energy of the electron beam is 230 eV

Figure 12: LEED patterns of Ni(100) after dosing CO and one cycle of cleaning

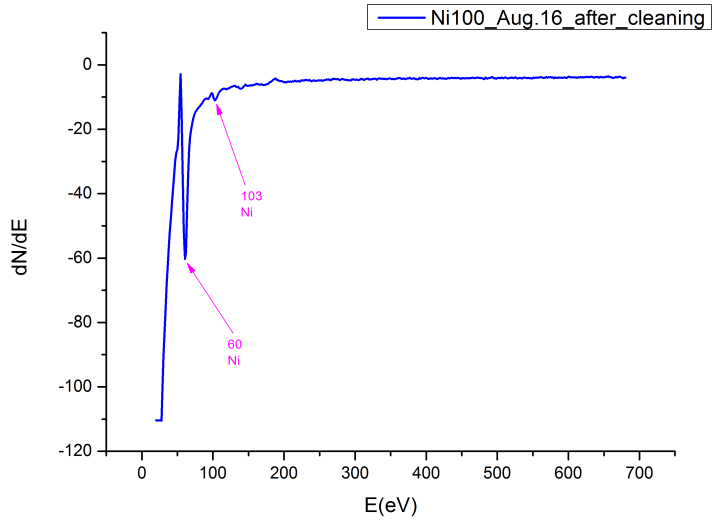

Figure 13: AES of Ni(100) after dosing and one cycle of cleaning.

The sample was cleaned by sputtering at room temperature for half an hour, followed by annealing up to 1400 K for 15 minutes under UHV conditions. Following information can be known from these LEED patterns. First, the surface is now clean from carbon and oxygen. When the electron energy is very low, as in Figure 12(a) and Figure 12(b), the twelve-fold pattern disappears, comparing with the LEED patterns taken directly after nickel was dosed CO (see Figure 10). So the spuerstructure formed by CO molecules doesn's exist any more. This point can be supported by the Auger spectrum taken after sputtering and heating in which no carbon or oxygen peak show up (see Figure 13). Second, the surface now is also clean from chlorine. From Figure 12(b), after some simple calculation, we can get that the d spacing is 2.37 Å, which is very

similar to the theoretical d spacing of Ni(100) 2.49 Å. This shows that the sharp spots in Figure 12(b) do come from Ni and no larger d spacing exists. From the Auger spectrum (Figure 13), no clorine peak can be seen, which supports the second point.

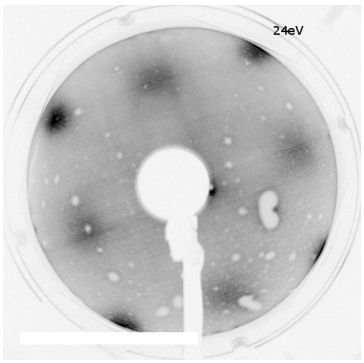

(a) Energy of the electron beam is 24 eV

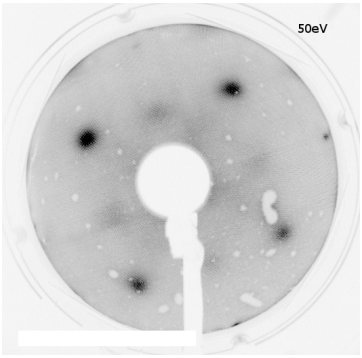

(b) Energy of the electron beam is 50 eV

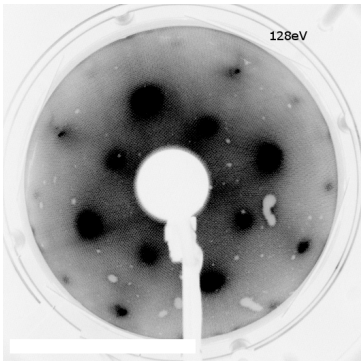

(c) Energy of the electron beam is 128 eV

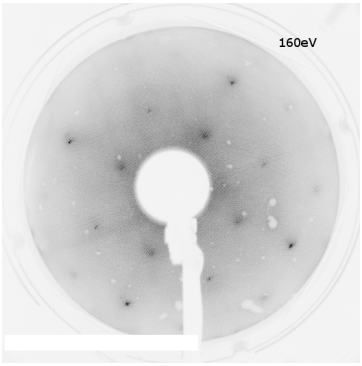

(d) Energy of the electron beam is 160 eV

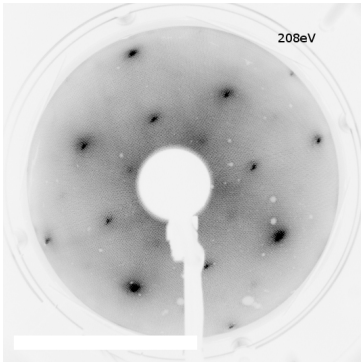

(e) Energy of the electron beam is 208 eV

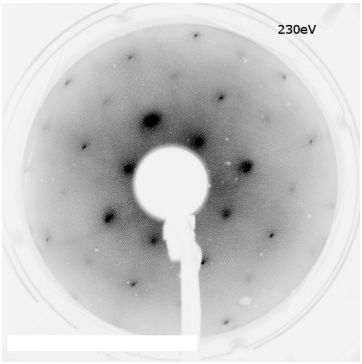

(f) Energy of the electron beam is 230 eV

Figure 14: LEED patterns of Ni(100) after the 2nd dosing CO and exposed to bad pressure

To repeat the CO dosing experiment, nickel was transfered to the IR chamber again. Unfortunately, after several cycles of dosing, there was a leak in on the tube between the CO leak valve and the IR UHV chamber. Nickel was exposed to bad pressure for three days. After the leak was fixed, nickel was transfered back into the main chamber, followed by taking LEED and AES. Figure 14 shows the LEED patterns of Ni(100) after the 2nd dosing CO and exposed to bad pressure. Figure 14(a) reveals a p(2×2) reconstruction.

4.2 IR Spectra and Analysis

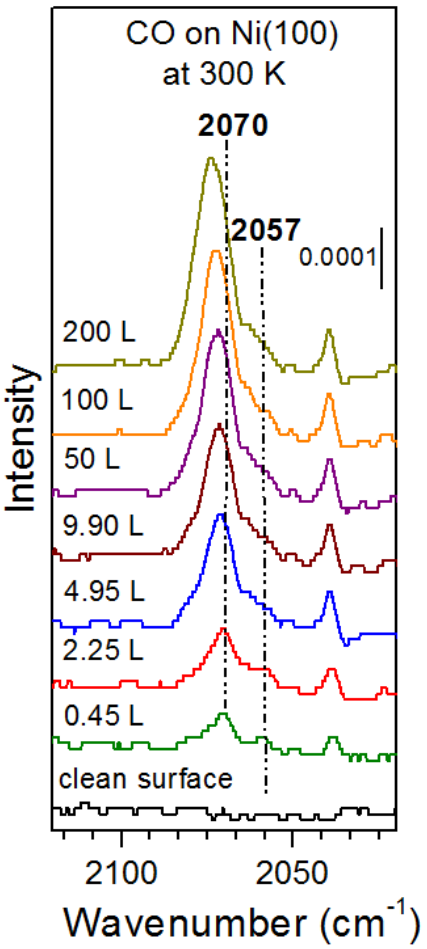

Figure 15: Series of infrared spectra of CO adsorption on Ni(100) at 200K for different exposures.

Figure 15 shows the IR spectra of CO adsorption on Ni(100) at 300K for different exposures. The CO peaks are between 2070 to 2075 cm^{-1}, which means the stretching energy of CO is around 257meV. These peaks may correspond to adsorption in on-top sites[10]. There is a series of peaks at lower wavenumber of 2035 cm^{-1}. The position

and intensity of this peak almost does not change with different exposures. So this peak can be regarded as a stable noise. Other methods, such as photoemission, are needed to establish which adsorption sites are occupied on a surface with nore than one possible adsorption geometry.

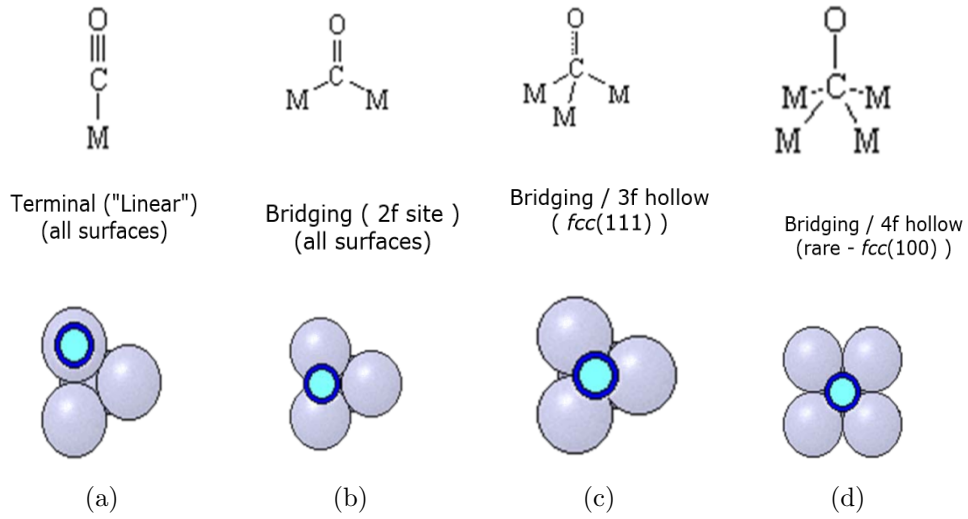

Figure 16: Four adsorption sites of CO on metal single crystal surface

As the exposure increases, we observe a blue shift from 2070 to 2075 cm^{-1}. The shift in the internal CO stretching vibration frequency may arise from a considerable lateral dipole-dipole interaction betwween adjacent CO molecules[7]. As the packing density of CO increases, there is an enhancement in the dipole coupling between the CO molecules in the surface and a weakening of their bonds to the metal, resulting in the observed frequency shift[8].

5 Conclusions

The whole story of Ni(100) studied in this report is as follows. Five cycles of sputtering and heating was conducted in the main chamber and a clean and well ordered surface was expected. However, on the well ordered surface, a c(2×2) reconstruction was observed. It is likely that chlorine formed the reconstruction. Then the sample was transfered to the IR chamber to be exposed to different Langmuirs of CO, each followed by taking IR spectra (see Figure 15). From the IR spectra we know that the CO stretching energy is 257 meV, which may correspond to the on-top adsorption. Then Ni(100) was transfered back to the main chamber aiming at to get some knowledge of the surface after dosing CO. From the LEED patterns, a superstructure induced by oxygen can be seen, which is supported by the oxygen peak in the AES. After that, the sample was cleaned by one cycle of sputtering and heating, then we get real clean surface without carbon, oxygen, and chlorine. Then Ni(100) was transfered to the IR chamber again, followed by a leak in the tube between the leak valve of CO and the IR

UHV chamber. P(2×2) reconstruction was observed after the sample was exposed to bad pressure.

Acknowledgement

The author gratefully acknowledge Andreas Stierle, Vedran Vonk and Heshmat Noei for their supervising, intensive discussions and valuable suggestions. The auther also thanks Riccardo Pisoni for his friendly coorporation and discussion.

References

[1] Growth and oxidation processes of Pt nanoparticles. *Uta Hejral*

[2] Adsorption of hydrogen on nickel single crystal surfaces. *K. Christmann, O. Schober, G. Ertl, and M. Neumann*

[3] Methods for the determination of trace impurities in nickel: boron, chloride, sulfide and sulfate. *Ram D. Srivastava and Hyman Gesser*

[4] Growth of thin, crystalline oxide, nitride and oxynitride films on metal and metal alloy surfaces. *Rene Franchy*

[5] Vibrational spectroscopic studies on adsorption and reactions over ZnO-based catalysts. *Heshmat Noei*

[6] On the structure of dense CO overlayers. *P. Uvdal, P. A. Karlsson, C. Nyberg, S. Andersson*

[7] Site occupation of CO adsorbed on Ni(100) at high CO pressures. *A. Grossmann, W. Erley, H. Ibach*

[8] CO adsorption on Ni(100) and Pt(111) studied by infrared-visible sum frequency generation spectroscopy: design and application of an SFG-compatible UHV-high-pressure reaction cell. *G. Rupprechter, T. Dellwig, H. Unterhalt and H. J. Freund*

[9] Surface oxides on close-packed surfaces of late transition metals. *Edvin Lundgren, Anders Mikkelsen, Jesper N Andersen, Georg Kresse, Michael Schmid and Peeter Varga*

[10] An IR reflection-absorption study of the CO/Ni(100) adsorption system. *R. Klauser, W. Spiess, A. M. Bradshaw and B. E. Hayden*